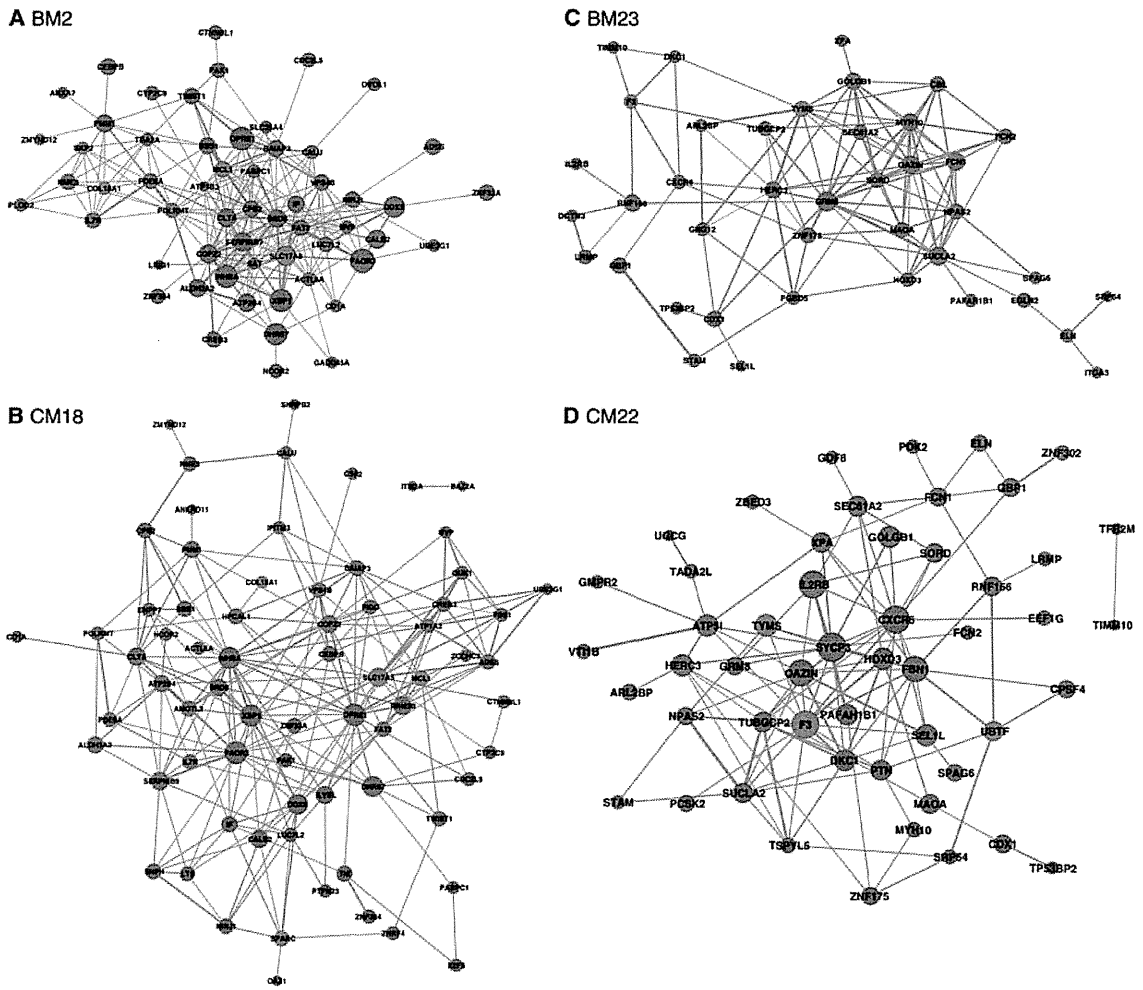

Figure 7 Topology of two pairs of overlapping HBV and HCV modules. For clarity, only the edges corresponding to top 5% correlations are shown. The node size corresponds to within-module connectivity, and the edge width corresponds to absolute value of correlation. Candidate HCC genes curated from literature are marked as red. For the BM2-CM18 pair, corresponds to the overlapping part in BM2 (**A**) and CM18 (**B**). For the BM23-CM22 pair, corresponds to the overlapping part in BM23 (**C**) and CM22 (**D**).

Another of our discoveries is that in both of the oncogenic HCV modules (namely, CM18, red, and CM22, turquoise), immune response (CM18, HCV, red, 9.55E−4) and inflammatory response (CM22, HCV, turquoise, 1.61E−5) were top enriched. Previous research reported that immune response and inflammatory phenotypes are predominant in HCV compared with HBV (Iizuka et al., 2002; Honda et al., 2006), and our result further suggested that compared with HBV-HCC, these two processes are more likely to be oncogenic for HCV-HCC. The HCV oncogenic module was uniquely enriched in lipid storage (CM22, HCV, turquoise, 0.0026) and previous findings also reported that lipid metabolism (Ura et al., 2009) is activated in HCV but not in HBV.

We also investigated the inflammation-related dysfunctional modules, because they represent tumor-suppressive processes that are disrupted upon cancer transformation. We observed that DNA damage response and signal transduction were uniquely enriched in the HBV dysfunctional module (BM9, HBV, darkred, 6.68E−3), and this is in concordance with previous research findings that DNA damage and signal transduction pathways are activated in HBV but not in HCV (Honda et al., 2006; Ura et al., 2009). In HCV dysfunctional modules, epithelial cell proliferation (CM23, HCV, yellow, 5.19E−5) was top enriched, which may be related to response to chronic inflammation upon HCV infection.

Different cellular processes and pathways represented by human protein targets of HBV and HCV

Beyond investigating the similarities and differences in these inflammation-related HBV and HCV modules in terms of gene compositions and functional annotations as well as dysfunctional implications, we attempted to provide a root cause analysis by exploring the human protein targets of HBV and HCV. Given that infection with HBV or HCV is one of the major risk factors contributing to HCC (Tsai and Chung, 2010), we considered whether it is the similarities and differences in viral targets of human proteins that explain the observed results. We constructed two interactome networks for human proteins interacting with HBV or HCV proteins (Supplementary Figure S1). The HCV interactome,

consisting of 11 HCV proteins and 481 human proteins, was generated from both Y2H assay and literature text-mining (de Chassey et al., 2008), and the HBV interactome, consisting of 5 HBV proteins and 250 human proteins, was generated from text-mining (Wu et al., 2010). We analyzed the pathway enrichment for each interactome to check whether HBV and HCV human protein targets correspond to distinct cellular pathways. A full list of enriched pathways and their gene compositions for HBV and HCV human protein targets is provided in Supplementary Tables S5 and S6, respectively. To analyze common and distinct cellular pathways represented by the two interactomes in a clear manner, we grouped annotations into clusters according to their semantic similarity (Kappa similarity threshold = 0.4) and ranked these functional annotation clusters (see Materials and methods for details). HBV human protein targets were found to be enriched in cancer pathways (rank 1, score = 5.08), inflammatory/immune pathways (rank 2, score = 3.1), and apoptosis signaling pathways (rank 3, score = 2.85). The HCV human protein targets were found to be enriched in cell surface interactions (rank 1, score = 5.03), and cancer pathways (rank 3, score = 1.51; Table 2). A detailed characterization of the functional annotation clusters is also provided in Supplementary Tables S5 and S6. Thus, we found that the cancer pathway is shared by two interactomes, but the HBV interactome is most enriched in apoptosis and the inflammatory/immune pathway while the HCV interactome is most enriched in cell surface interactions and the cell cycle.

The difference in annotated clusters between HBV and HCV interactome was confirmed by the distinct life cycles of HBV and HCV. HBV is non-cytopathic, and only its encapsulated DNA genome can be transported into the cell (Seeger et al., 2007). The virus-induced liver injury is associated with the influx of immune cells into the liver and the destruction of HBV-infected hepatocytes (Guidotti et al., 1999). Integration of viral DNA into the host genome can induce DNA recombination and damage (Bonilla Guerrero and Roberts, 2005). In contrast, HCV interacts with the host cell surface, and the whole virus is transported into the cell via receptor-mediated endocytosis (Blanchard et al., 2006). HCV is unable to reverse transcribe its RNA genome and thus unable to integrate into the host genome (Ashfaq et al., 2011). Our module-based approach not only re-addressed these aspects, but also identified pro-apoptosis and anti-apoptosis as the driving force of carcinogenesis in HBV and HCV, respectively, which cannot be revealed by viral target analysis.

Relating viral targets to the coexpression network, we are interested in protein targets, which belong to oncogenic modules. Although HBV and HCV viral targets have overlap, we found that none of the overlapping proteins belong to both HBV and HCV oncogenic modules (Table 1). In other words, HBV and HCV oncogenic modules each contain a disjoint set of target proteins. Supplementary Table S7 provides detailed information about human proteins targeted by HBV and HCV, their differential expression during disease progression and module memberships.

The KEGG database contains a pathway for Hepatitis C. Of the 134 genes contained in the Hepatitis C pathway, only 24 of them are direct targets of HCV. Functional annotation clusters showed that Hepatitis C is most enriched in the inflammatory/immune pathway (Table 2), which is different from HCV. One reason is that the upstream direct virus targets and their downstream response elements have different cellular functions. Another is that the Hepatitis C pathway is incomplete, and functions have not yet been attributed to all proteins. Besides comparing functional annotations of virus targets which represent initial perturbations, another powerful way to understand the different effects of HBV and HCV infections is to identify the response elements upon viral perturbations by analyzing gene expression profiles in our framework.

Discussion

We have conducted, to the best of our knowledge, the first comprehensive and comparative study of gene coexpression analysis at a network level to reveal the similarities and differences in HBV-HCC and HCV-HCC, in particular focusing on the inflammation-related analyses of viral infection. Our results demonstrate the advantages of a network-based systems biology approach over the previous differential expression approach and viral protein target-based approach. After validation by independent datasets, we identified 3 HBV and 2 HCV oncogenic modules, as well as 2 HBV and 2 HCV dysfunctional modules according to module preservation in normal livers and HCC. Those modules act as driving forces of carcinogenesis in HBV and HCV, respectively. The top enriched functional annotations of these modules are also in concordance with previous research and consistent with our existing knowledge of the distinct lifecycles of HBV and HCV in hepatocytes. In addition, the top enriched transmembrane transport and transmembrane receptor signaling pathway in one HBV oncogenic module suggested their potentially important roles in HBV-HCC.

Notably, our discoveries in distinct functional annotations represented by HBV and HCV modules could not have been revealed by existing standard methods such as differential expression and viral targets. First, we found no gene significantly differential expressed between HBV-infected and HCV-infected liver samples (Supplementary Table S8), rendering direct comparison of gene expression profiles in this status impossible. Second, we could not have selected those interesting inflammation-related modules and further classified them into four types without the use of module preservation in normal and HCC livers, which is also the advantage of our approach over other coexpression-based analysis of gene expression only in disease status, or disease vs control status (Ivliev et al., 2010). It should also be noted that if starting from modules in normal status, the viral infection oncogenic modules would be missed; and if starting from modules in HCC, the viral infection dysfunctional modules would be missed as well. Our theme is to identify these modules upon viral infection which we regarded as a process critical to HCC. Moreover, we narrowed down our analyses of these oncogenic and dysfunctional modules by considering all the combinatorial cases of module preservation in the three stages. The transit modules might particularly indicate the dysfunctional responses of virus infection, while we mainly focused on these repetitive modules in multiple disease progression stages. Third, we fully utilized the inherent variability in gene expression that exists in the same phenotype samples, and

further incorporated both the change of gene expression levels and the change of gene–gene coexpression relationships (i.e. connectivity) on the module level. By using a permutation-based approach, we eliminated the effect of different sample size between groups in the identification and comparison.

Materials and methods

Microarray data and workflow

Figure 1 shows the overview of our framework. A toy example of constructing gene coexpression network is illustrated in Figure 1A, our computational procedure is summarized in Figure 1B, and the module identification and classification of four types of modules are summarized in Figure 2. We analyzed four microarray datasets from independent studies, and a summary of the four datasets is described in Supplementary Table S1. The primary results were based on Kanazawa data (Honda et al., 2006; Ivliev et al., 2010). The other three datasets were mainly used for validation purposes. Both GSE14323 (Mas et al., 2009) and GSE19665 (Deng et al., 2010) were analyzed using the Affymetrix HG-U133A platform, and therefore, a probe set summary for each dataset was obtained using the RMA method in the affy package in R (Gautier et al., 2004). GSE3500 (Chen et al., 2002, 2004) was retrieved from the Stanford Microarray Database, using regression correlation. For GSE3500, samples and probe sets with >20% missing values were filtered, and the remaining missing values were imputed using impute package in R (Troyanskaya et al., 2001). When multiple probe sets were mapped to the same gene Entrez ID, the average expression vector was computed and used. Gene coexpression modules were identified from HBV- and HCV-infected liver samples, and validated on respective independent datasets. Only verified modules were used to analyze the dynamic change of modules during three stages of disease progression in HBV and HCV, respectively.

Weighted gene coexpression network construction and module identification

We built the weighted gene coexpression networks (Zhang and Horvath, 2005) for HBV and HCV by computing the gene correlation coexpression and inferring the coexpression networks in 36 HBV-infected samples and 35 HCV-infected samples, respectively. In a weighted gene coexpression network, the nodes represent genes and the edges represent the connection strength (adjacency), $a_{ij} = |\mathrm{cor}(x_i, x_j)|^{\beta}$, between the two gene expression profiles x_i and x_j. A major advantage of weighted networks is that the results are highly robust with regard to the choice of parameter β. Zhang and Horvath (2005) proposed a scale-free topology criterion for choosing β, and here we chose it to be six so that this yields approximately the same number of modules for HBV- and HCV-infected liver samples. The final adjacency was further transformed into a TO (Yip and Horvath, 2007). Then the modules were detected using the Dynamic Tree Cut algorithm (Langfelder et al., 2007; deep split = 2, cut height = 0.995, other parameters are defaulted).

As previously proposed, the module membership, k_{ME}, for each gene is defined as the Pearson's correlation between the expression level of the gene and the ME to which the gene belongs (Dong and Horvath, 2007). The k_{ME} for each gene was measured and the gene was assigned to the module which maximizes its k_{ME}. To avoid capturing weak associations, genes with $k_{ME} < 0.3$ for all of the MEs were assigned to none of them.

Functional annotation of gene sets and viral infection modules

Functional annotations of the gene sets and modules were performed on the basis of their gene composition using DAVID (http://david.abcc.ncifcrf.gov/). In DAVID, the reported *P*-values were derived from the EASE score probability, and a modified Fisher's exact test that is more conservative than the standard Fisher's exact test. 'BBID', 'BIOCARTA', 'KEGG_PATHWAY', 'PANTHER_PATHWAY', and 'REACTOME_PATHWAY' were selected for pathway enrichment analysis of viral protein targets. For characterization of modules, 'GO_BP_FAT' was selected. Due to the redundancy of annotations, similar or relevant annotations often appear repeatedly. We also adopted the functional annotation clustering provided in DAVID to help focus on biology in our study. We set the classification stringency to Medium, and clusters were ranked according to their *P*-values, which have exactly the same meaning as *P*-values for individual terms, and a false discovery rate (FDR) accompanying with each term was also reported.

Module internal validation and external validation

The purpose of internal validation is to rule out the possibility that some modules are based on gene coexpression across the full set of samples whereas others are the result of coordinate gene regulation in a subset of samples. Co-clustering statistics (Langfelder et al., 2011) is a cross-tabulation-based statistics for determining whether modules in the reference dataset are preserved in a test dataset. Reference modules are labeled $q = 1, 2, \ldots, Q^{[\mathrm{ref}]}$, test modules are labeled $q\prime = 1, 2, \ldots, Q^{[\mathrm{test}]}$, and the number of genes in module q or $q\prime$ is denoted by $n^{(q)}$ or $n^{(q\prime)}$. For HBV and HCV, respectively, we randomly chose 70% samples and identified modules, using the same procedure as described above, and iterated the random sampling and module identification process 100 times and generated 100 sets of test modules, $\{q\prime_i, i = 1, \ldots, 100\}$. For each set of modules, we computed its co-clustering statistics with reference modules, q (modules identified from full set of samples). The proportion of pairs of genes in both module q and module q' is given by $propCoClustering(q, q\prime) = \binom{n_{qq\prime}}{2} / \binom{n^{(q)}}{2}$, where $n_{qq\prime}$ is defined as the number of genes that are both in the reference module q and in the test module $q\prime$, the co-clustering statistics for module q is defined as the sum of the above proportions over all clusters $q\prime$ in the test clustering, $coClustering(q) = \sum_{q\prime=1}^{Q^{[\mathrm{test}]}} propCoClustering(q, q\prime)$. Then, a permutation test for 100 times was conducted for each test set of modules to determine whether the observed co-clustering statistics are significantly different from those expected by chance. Finally, we selected the reference modules with significant co-clustering statistics in 95% of the test sets.

To validate the reproducibility of modules in independent datasets, we identified coexpression modules in independent datasets (GSE14323 for HCV and GSE3500 for HBV individually) using the same procedures as described above and

extracting the common genes shared by two datasets, then we computed the significance of module overlap based on the Fisher's exact test using the common genes and their module memberships.

Module preservation in different disease stages

To capture both the dynamics of individual gene expression and the dynamics of gene–gene correlation coexpression relationship (Miller et al., 2010) between disease stages as shown in Figure 5, for each module we analyzed the enrichment of differentially expressed genes and the preservation of coexpression network topology using the permutation-based approach.

First, DE genes, $\{g_j\}$ (adjusted P-value < 0.05), were identified using the lmFit function provided in the R limma package (Smyth, 2004), and a t-score was assigned to each gene that quantified the significance of DE between phenotypes. A full list recording the significance of differential expression for each gene, normal vs viral infection and viral infection vs HCC, is provided in Supplementary Table S8. For each module, an average t-score was computed by dividing the sum of individual t-score by module size, $t\text{-score}(M_i) = \left(\sum_{g_j \in M_i} |t\text{-score}(g_j)|\right)/\text{size}(M_i)$. The significance of DE enrichment is given by the proportion of 1000 permutations in which random modules of the same size associated with a larger t-score than the reference module.

To evaluate the preservation of modules between two gene coexpression networks, N_l and N_m, constructed from samples of different size, we adopted a previous measure of intramodular connectivity preservation (Dewey et al., 2011). We first computed the intramodular connectivity (Dong and Horvath, 2007) vectors k^l and k^m, where $k = \left\{k_i : k_i = \sum_{j \neq i}^{i,j \in M} a_{ij}\right\}$, k_i is the intramodular connectivity of node i, a_{ij} is the adjacency, and nodes i and j belong to the same module M. Then for each module M_j, $M_j \in M$, we computed its intramodular connectivity preservation $\text{Pres}^{l,m}_{M_j} = \text{cor}(k^l_{i \in M_j}, k^m_{i \in M_j})$. Under the null hypothesis that the derived module, M_j, is preserved between N_l and N_m no better than modules derived from random clustering, we randomly permuted gene labels so that modules of the same size but random gene composition were generated. 1000 such permutations were performed, and the proportion of permutations in which $\text{Pres}^{l,m}_{M_{\text{rand}}} > \text{Pres}^{l,m}_{M_j}$ was used to evaluate the significance of test. Such a test was used to evaluate the preservation of modules in normal and HCC, for HBV- and HCV-liver samples, respectively. Since samples in viral-infected liver tissue consist of four stages of fibrosis, we also computed the enrichment of genes significantly correlated with fibrosis for each module using similar statistics as described above, where $\text{cor}(M_i) = \left(\sum_{g_j \in M_i} |\text{cor}(g_j)|\right)/\text{size}(M_i)$.

Supplementary material

Supplementary material is available at *Journal of Molecular Cell Biology* online.

Acknowledgements

We thank Dr Katsuhisa Horimoto of National Institute of Advanced Industrial Science and Technology, Japan for his kindly help.

Funding

This work was supported by the NSFC (Nos. 31100949, 91029301, 61134013 and 61072149), the Chief Scientist Program of Shanghai Institutes for Biological Sciences (SIBS), Chinese Academy of Sciences (CAS) (No. 2009CSP002), Shanghai NSF (No. 11ZR1443100) and the Knowledge Innovation Program of SIBS of CAS (No. 2011KIP203) and the SA-SIBS Scholarship Program. This research was also partially supported by the National Center for Mathematics and Interdisciplinary Sciences of CAS, Shanghai Pujiang Program, and the FIRST program from JSPS initiated by CSTP.

Conflict of interest: none declared.

References

Alexandros, K., and David, M. (2006). Support vector machines in R. J Stat. Softw. *15*, 9.

Ashfaq, U.A., Javed, T., Rehman, S., et al. (2011). An overview of HCV molecular biology, replication and immune responses. Virol. J *8*, 161.

Blanchard, E., Belouzard, S., Goueslain, L., et al. (2006). Hepatitis C virus entry depends on clathrin-mediated endocytosis. Virol. J. *80*, 6964–6972.

Bonilla Guerrero, R., and Roberts, L.R. (2005). The role of hepatitis B virus integrations in the pathogenesis of human hepatocellular carcinoma. J. Hepatol. *42*, 760–777.

Bouchard, M.J., and Navas-Martin, S. (2011). Hepatitis B and C virus hepatocarcinogenesis: lessons learned and future challenges. Cancer Lett. *305*, 123–143.

Chen, X., Cheung, S.T., So, S., et al. (2002). Gene expression patterns in human liver cancers. Mol. Biol. Cell *13*, 1929–1939.

Chen, X., Higgins, J., Cheung, S.T., et al. (2004). Novel endothelial cell markers in hepatocellular carcinoma. Mod. Pathol. *17*, 1198–1210.

Chen, L., Wang, R.S., and Zhang, X.S. (2009). Biomolecular Networks: Methods and Applications in Systems Biology. New Jersey: John Wiley & Sons, Inc.

Chen, L., Liu, R., Liu, Z.P., et al. (2012). Detecting early-warning signals for sudden deterioration of complex diseases by dynamical network biomarkers. Sci. Rep. *2*, 342.

Chung, Y.L., Sheu, M.L., and Yen, S.H. (2003). Hepatitis C virus NS5A as a potential viral Bcl-2 homologue interacts with Bax and inhibits apoptosis in hepatocellular carcinoma. Int. J. Cancer *107*, 65–73.

de Chassey, B., Navratil, V., Tafforeau, L., et al. (2008). Hepatitis C virus infection protein network. Mol. Syst. Biol. *4*, 230.

Deng, Y.B., Nagae, G., Midorikawa, Y., et al. (2010). Identification of genes preferentially methylated in hepatitis C virus-related hepatocellular carcinoma. Cancer Sci. *101*, 1501–1510.

Dewey, F.E., Perez, M.V., Wheeler, M.T., et al. (2011). Gene coexpression network topology of cardiac development, hypertrophy, and failure. Circ. Cardiovasc. Genet. *4*, 26–35.

Dong, J., and Horvath, S. (2007). Understanding network concepts in modules. BMC Syst. Biol. *1*, 24.

Gautier, L., Cope, L., Bolstad, B.M., et al. (2004). affy—analysis of Affymetrix GeneChip data at the probe level. Bioinformatics *20*, 307–315.

Guidotti, L.G., Rochford, R., Chung, J., et al. (1999). Viral clearance without destruction of infected cells during acute HBV infection. Science *284*, 825–829.

Honda, M., Yamashita, T., Ueda, T., et al. (2006). Different signaling pathways in the livers of patients with chronic hepatitis B or chronic hepatitis C. Hepatology *44*, 1122–1138.

Iizuka, N., Oka, M., Mori, N., et al. (2002). Comparison of gene expression profiles between hepatitis B virus- and hepatitis C virus-infected hepatocellular carcinoma by oligonucleotide microarray data on the basis of a supervised learning method. Cancer Res. *62*, 3939–3944.

Ivliev, A.E., 't Hoen, P.A., and Sergeeva, M.G. (2010). Coexpression network analysis identifies transcriptional modules related to proastrocytic

differentiation and sprouty signaling in glioma. Cancer Res. *70*, 10060–10070.

Lan, K.H., Sheu, M.L., Hwang, S.J., et al. (2002). HCV NS6A interacts with p53 and inhibits p53-mediated apoptosis. Oncogene *21*, 4801–4811.

Langfelder, P., Zhang, B., and Horvath, S. (2007). Defining clusters from a hierarchical cluster tree: the Dynamic Tree Cut library for R. Bioinformatics *24*, 719–720.

Langfelder, P., Luo, R., Oldham, M.C., et al. (2011). Is my network module preserved and reproducible? PLoS Comput. Biol. *7*, e1001057.

Liu, Z.P., Wang, Y., Zhang, X.S., et al. (2012). Network-based analysis of complex diseases. IET Syst. Biol. *6*, 22–33.

Mas, V.R., Maluf, D.G., Archer, K.J., et al. (2009). Genes involved in viral carcinogenesis and tumor initiation in hepatitis C virus-induced hepatocellular carcinoma. Mol. Med. *15*, 85–94.

Miller, J.A., Horvath, S., and Geschwind, D.H. (2010). Divergence of human and mouse brain transcriptome highlights Alzheimer disease pathways. Proc. Natl Acad. Sci. USA *107*, 12698–12703.

Oldham, M.C., Konopka, G., Iwamoto, K., et al. (2008). Functional organization of the transcriptome in human brain. Nat. Neurosci. *11*, 1271–1282.

Perz, J.F., Armstrong, G.L., Farrington, L.A., et al. (2006). The contributions of hepatitis B virus and hepatitis C virus infections to cirrhosis and primary liver cancer worldwide. J. Hepatol. *45*, 529–538.

Rabe, B., Delaleau, M., Bischof, A., et al. (2009). Nuclear entry of hepatitis B virus capsids involves disintegration to protein dimers followed by nuclear reassociation to capsids. PLoS Pathog. *5*, e1000563.

Ravasz, E., Somera, A.L., Mongru, D.A., et al. (2002). Hierarchical organization of modularity in metabolic networks. Science *297*, 1551–1555.

Seeger, C., Zoulim, F., and Mason, W.S. (2007). Fields Virology. Philadelphia: Lippincott Williams & Wilkins.

Smyth, G.K. (2004). Linear models and empirical Bayes methods for assessing differential expression in microarray experiments. Stat. Appl. Genet. Mol. Biol. *3*, Article 3.

Stuart, J.M., Segal, E., Koller, D., et al. (2003). A gene-coexpression network for global discovery of conserved genetic modules. Science *202*, 249–255.

Troyanskaya, O., Cantor, M., Sherlock, G., et al. (2001). Missing value estimation methods for DNA microarrays. Bioinformatics *17*, 520–525.

Tsai, W.L., and Chung, R.T. (2010). Viral hepatocarcinogenesis. Oncogene *29*, 2309–2324.

Ura, S., Honda, M., Yamashita, T., et al. (2009). Differential microRNA expression between hepatitis B and hepatitis C leading disease progression to hepatocellular carcinoma. Hepatology *49*, 1098–1112.

Wang, H., He, X., Band, M., et al. (2005). A study of inter-lab and inter-platform agreement of DNA microarray data. BMC Genomics *6*, 71.

Wu, Z.J., Zhu, Y., Huang, D.R., et al. (2010). Constructing the HBV-human protein interaction network to understand the relationship between HBV and hepatocellular carcinoma. J. Exp. Clin. Cancer Res. *29*, 146.

Wurmbach, E., Chen, Y.B., Khitrov, G., et al. (2007). Genome-wide molecular profiles of HCV-induced dysplasia and hepatocellular carcinoma. Hepatology *45*, 938–947.

Yip, A., and Horvath, S. (2007). Gene network interconnectedness and the generalized topological overlap measure. BMC Bioinf. *8*, 22.

Zhang, B., and Horvath, S. (2005). A general framework for weighted gene co-expression network analysis. Stat. Appl. Genet. Mol. Biol. *4*, Article 17.

J Gastroenterol
DOI 10.1007/s00535-012-0596-x

ORIGINAL ARTICLE—LIVER, PANCREAS, AND BILIARY TRACT

Sequential immunological analysis of HBV/HCV co-infected patients during Peg-IFN/RBV therapy

Yasuteru Kondo · Yoshiyuki Ueno · Masashi Ninomiya · Keiichi Tamai · Yasuhito Tanaka · Jun Inoue · Eiji Kakazu · Koju Kobayashi · Osamu Kimura · Masahito Miura · Takeshi Yamamoto · Tomoo Kobayashi · Takehiko Igarashi · Tooru Shimosegawa

Received: 29 August 2011 / Accepted: 28 March 2012

Abstract

Background The immunopathogenesis of dual chronic infection with hepatitis B virus and hepatitis C virus (HBV/HCV) remains unclear. The in vivo suppressive effects of each virus on the other have been reported. In this study we aimed to analyze the virological and immunological parameters of HBV/HCV coinfected patients during pegylated interferon/ribavirin (Peg-IFN/RBV) therapy.

Methods One patient with high HBV-DNA and high HCV-RNA titers (HBV-high/HCV-high) and 5 patients with low HBV-DNA and high HCV-RNA titers (HBV-low/HCV-high) were enrolled. Twenty patients monoinfected with HBV and 10 patients monoinfected with HCV were enrolled as control subjects.. In vitro cultures of Huh 7 cells with HBV/HCV dual infection were used to analyze the direct interaction of HBV/HCV.

Results Direct interaction of HBV clones and HCV could not be detected in the Huh-7 cells. In the HBV-high/HCV-high-patient, the HCV-RNA level gradually declined and HBV-DNA gradually increased during Peg-IFN/RBV therapy. Activated CD4- and CD8-positive T cells were increased at 1 month of Peg-IFN/RBV-therapy, but HBV-specific IFN-γ-secreting cells were not increased and HBV-specific interleukin (IL)-10 secreting cells were increased. The level of HBV- and HCV-specific IFN-γ-secreting cells in the HBV-high/HCV-high-patient was low in comparison to that in the HBV- or HCV-monoinfected patients. In the HBV-low/HCV-high-patient, HCV-RNA and HBV-DNA rapidly declined during Peg-IFN/RBV therapy. Activated CD4- and CD8-positive T cells were increased, and HBV- and HCV-specific IFN-γ-secreting cells were also increased during Peg-IFN/RBV-therapy.

Conclusion The immunological responses of the HBV-high/HCV-high patient were low in comparison to the responses in HBV and HCV monoinfected patients. Moreover, the response of immune cells in the HBV-high/HCV-high patient during Peg-IFN/RBV therapy was insufficient to suppress HBV and HCV.

Keywords Dual infection · HBV · HCV · Immunopathogenesis

Electronic supplementary material The online version of this article (doi:10.1007/s00535-012-0596-x) contains supplementary material, which is available to authorized users.

Y. Kondo · Y. Ueno (✉) · M. Ninomiya · K. Tamai · J. Inoue · E. Kakazu · O. Kimura · T. Shimosegawa
Division of Gastroenterology, Tohoku University Graduate School of Medicine, 1-1 Seiryo, Aobaku, Sendai, Miyagi, Japan
e-mail: y-ueno@med.id.yamagata-u.ac.jp; yeuno@med.tohoku.ac.jp

Y. Tanaka
Virology and Liver Unit, Nagoya City University Medical School, Nagoya, Japan

K. Kobayashi
Tohoku University Graduate School of Medicine, 2-1 Seiryo, Aobaku, Sendai, Miyagi, Japan

M. Miura
Department of Gastroenterology, South Miyagi Medical Center, Oogawara, Miyagi, Japan

T. Yamamoto
Department of Gastroenterology, Tohoku Kosei-Nenkin Hospital, Sendai, Miyagi, Japan

T. Kobayashi
Department of Hepatology, Tohoku Rosai Hospital, Sendai, Miyagi, Japan

T. Igarashi
Department of Gastroenterology, Osaki Citizen Hospital, Osaki, Japan

Published online: 16 May 2012

Introduction

Hepatitis B virus (HBV) and Hepatitis C virus (HCV) are noncytopathic viruses that cause chronic hepatitis and hepatocellular carcinoma (HCC) [1, 2]. HBV now affects more than 400 million people worldwide, and persistent infection develops in ~5 % of adults and 95 % of neonates who become infected with HBV [3]. HCV infects about 170 million people worldwide and is a major cause of chronic hepatitis, cirrhosis, and HCC [4]. Some groups have mentioned that dual infection with HBV/HCV is not uncommon in Asian patients [5, 6]. The prevalence of patients with dual HBV/HCV infection is approximately 10–15 %, although it likely differs among countries [7–9]. Co-infection with HBV/HCV has been associated with severe liver disease and frequent progression to cirrhosis [10]. Moreover, a significantly higher incidence of HCC and liver-related mortality was noted in patients with HBV/HCV co-infection [11, 12]. However, some groups reported, based on a meta-analysis, that dual infection with HBV/HCV did not increase the risk of HCC [13, 14]. These contradictory reports could be explained by the rarity of dual infection with HBV/HCV in patients without clinically evident liver disease. It might be difficult to estimate the hepatocarcinogenic risk of dual infection compared with that of either infection alone in such clinical settings [15].

An inverse relationship in the replicative levels of the two viruses has been noted, suggesting direct or indirect effects in vivo [16]. More recently, some groups have reported, using an in vitro infection system, that there is little direct interaction of HBV/HCV in coinfected hepatocytes [17, 18]. Therefore, the viral interference observed in coinfected patients is probably due to indirect mechanisms mediated by the innate and/or adaptive host immune responses.

The cellular immune response to HBV and HCV plays an important role in the pathogenesis of chronic hepatitis, cirrhosis, and HCC [19–21]. Hyporesponsiveness of HBV- or HCV-specific T-helper 1 cells and excessive regulatory function of $CD4^+CD25^+FoxP3^+$ regulatory T cells (Tregs) in peripheral blood have been shown in patients with chronic hepatitis B and C [22–34]. Recently, we reported that HBV replication stress could enhance the suppressive activity of Tregs via TLR2 [35]. However, little is known about the immunopathogenesis of HBV/HCV dual infection.

Dual infection can be classified into several groups (e.g., group A: HBV active and HCV active; group B: HBV inactive and HCV active; and group C: HBV active and HCV inactive) [36]. HCV is reported to be the dominant virus in HBV/HCV dual infection, but the dominance of either virus might be due to the genotypes of each virus and/or ethnic differences that could affect the proliferative activity of the viruses [36]. In this study, we investigated immunopathogenesis in a group A patient and in group B patients during therapy with pegylated interferon-α2b (Peg-IFN-α2b) plus ribavirin.

Patients, materials, and methods

Patients

One patient with high HBV-DNA and high HCV-RNA titers (HBV-high/HCV-high; patient A) and 5 patients with low HBV-DNA and high HCV-RNA titers (HBV-low/HCV-high) were enrolled (one of these patients, whose results were analyzed in detail, was termed patient B; see findings below in the "Results"). Twenty patients monoinfected with HBV and 10 patients monoinfected with HCV were enrolled as control subjects. None of the patients had liver disease due to other causes, such as alcohol, drugs, congestive heart failure, or autoimmune diseases. Permission for the study was obtained from the Ethics Committee at Tohoku University Graduate School of Medicine (permission no. 2006-194). Written informed consent was obtained from all the participants enrolled in this study. Participants were monitored for two years. At each assessment, patients were evaluated by biochemical laboratory tests, immunological analysis, and virological tests. Liver histology was analyzed at the start of Peg-IFN/RBV therapy by using laparoscopic liver biopsy samples and by employment of the METAVIR score.

Detection of interleukin (IL)-28B polymorphism

Genomic DNA was isolated from peripheral blood mononuclear cells (PBMCs) using an automated DNA isolation kit. Then polymorphism of IL-28B (rs8099917) was analyzed using real-time polymerase chain reaction (PCR) (TaqMan SNP Genotyping Assay, Applied Biosystems, CA, USA). Detection of the IL-28B polymorphism was approved by the Ethics Committee at Tohoku University Graduate School of Medicine (permission no. 2010-323).

Isolation of peripheral blood mononuclear cells (PBMCs) and flow cytometry

Peripheral blood mononuclear cells (PBMCs) were isolated from fresh heparinized blood by means of Ficoll-Hypaque density gradient centrifugation (Amersham Bioscience, Uppsala, Sweden). PBMCs were stained with CD3, CD4, CD8, CD19, CD25, CD40, CD56, CD86, HLA-DR, NKG2D, and isotype control antibodies (Becton Dickinson, NJ, USA) for 15 min on ice to analyze the frequency

of $CD3^+CD4^+HLA\text{-}DR^+$ cells, $CD3^+CD8^+HLA\text{-}DR^+$ cells, $CD4^+CD25^+$ Tregs, $CD3^-CD16^-CD56^{high}$ natural killer (NK) cells, and $CD3^-CD16^+CD56^{dim}$ NK cells. The frequencies of the immune subsets were analyzed by flow cytometry using FACS Canto-II (Becton Dickinson, NJ, USA).

ELISPOT assay

The detection of IFN-γ and IL-10 was performed using an ELISPOT Set (BD Biosciences, San Jose, CA, USA) according to the manufacturer's instructions. Cultures of PBMCs were established in triplicate on round-bottomed 96-well plates for all time points investigated, at a concentration of 3×10^5 cells per well in 100 µl RPMI 1640 containing 10 % fetal bovine serum (FBS). Positive spots were detected using an automated counting machine.

Detection of HBV-DNA and determination of HBV genotype

DNA was extracted from 100 µl of serum using SMITEST EX-R&D (Medical & Biological Laboratories, Nagoya, Japan) and dissolved in 20 µl of nuclease-free distilled water. The DNA preparation thus obtained (10 µl) was subjected to nested PCR with primers targeting the S gene of the HBV-DNA, as described previously [37]. Briefly, first-round PCR was carried out for 35 cycles (98 °C for 10 s, 55 °C for 15 s, and 72 °C for 1 min, with an additional 7 min in the last cycle) in the presence of PrimeSTAR HS DNA Polymerase (TaKaRa Bio, Shiga, Japan) and primers HB095 (sense, 5′-GAG TCT AGA CTC GTG GTG GAC-3′) and HB184 (antisense, 5′-CGA ACC ACT GAA CAA ATG GCA CCG-3′), for 25 cycles. This was followed by a second-round PCR consisting of 25 cycles using the same conditions as in the first round, with primers HB097 (sense, 5′-GAC TCG TGG TGG ACT TCT CTC-3′) and S2-2 (antisense, 5′-GGC ACT AGT AAA CTG AGC CA-3′). The HBV genotype was determined by phylogenetic analysis of the S gene sequence (437 nt) of the HBV isolates.

Detection of HCV RNA

RNAs were extracted from 250 µl of serum using TRIzol LS (Invitrogen, Tokyo, Japan). They were divided into two aliquots and each was assayed by reverse transcription (RT)-PCR with nested primers derived from the core region and NS5A interferon sensitivity determining region (ISDR) of the HCV genome. Nested PCR of the core region of the HCV genome was carried out with primers C008 (sense, 5′-AAC CTC AAA GAA AAA CCA AAC G-3′) and C011 (antisense, 5′-CAT GGG GTA CAT YCC GCT YG-3′) in the first round and C009 (sense, 5′-CCA CAG GAC GTY AAG TTC CC-3′) and C010 (antisense, 5′-AGG GTA TCG ATG ACC TTA CC-3′) in the second round. Nested primers that were derived from NS5A-ISDR of the HCV genomes were designed to amplify a 188-bp product with C004 (sense, 5′-ATG CCC ATG CCA GGT TCC AG-3′) and C005 (antisense, 5′-AGC TCC GCC AAG GCA GAA GA-3′) in the first round, and C006 (sense, 5′-ACC GG A TGT GGC AGT GCT CA-3′) and C007 (antisense, 5′-GTA ATC CGG GCG TGC CCA TA-3′) in the second round.

Analysis of nucleotide and amino acid sequences

The PCR products were sequenced directly on both strands using a BigDye Terminator version 3.1 Cycle Sequencing Kit on an ABI PRISM 3100 Genetic Analyzer (Applied Biosystems, Foster City, CA, USA). Sequence analysis was performed using Genetyx-Mac ver. 12.2.6 (Genetyx, Tokyo, Japan) and ODEN (version 1.1.1) from the DNA Data Bank of Japan (National Institute of Genetics, Mishima, Japan) [38]. Sequence alignments were generated using CLUSTAL W (Version 1.8) [39]. The phylogenetic tree was constructed by the neighbor-joining method [40]. The reliability of the phylogenetic results was assessed using 1000 bootstrap replicants [41]. The final tree was obtained with the Njplot program (version 2.2) [42].

Plasmid construction

HBV expression plasmids were constructed by previously published methods. Serum samples were obtained from two patients infected with HBV genotype Bj and two patients infected with HBV genotype C. HBV-DNA was extracted from 100 µl serum using a QIAamp DNA blood kit (QIAGEN, Hilden, Germany). Four primer sets were designed to amplify two fragments covering the entire HBV genome. Amplified fragments were inserted into a pGEM-T Easy Vector (Promega, Madison, WI, USA) and cloned in DH5a competent cells (TOYOBO, Osaka, Japan). Briefly, at least 5 clones of each fragment were sequenced and the consensus sequence was identified and used as a template for 1.24-fold the HBV genome of different genotypes (B1 indicates the genotype Bj35 clone; B2 indicates the genotype Bj56 clone; C1 indicates the genotype C-AT clone; and C2 indicates the genotype C-22 clone). The HCV-JFH-1 strain was provided by Dr. T. Wakita (National Institute of Infectious Diseases, Japan).

HCV and HBV expression in Huh 7 cells

Cell-culture-derived infectious HCV was generated as described previously [43]. The HCV was quantified as

follows: RNA was extracted from the Huh-7 culture supernatant using a QIAamp Viral RNA Kit (Qiagen, Valencia, CA, USA). The HCV RNA was quantified by real-time RT-PCR, using TaqMan EZ RT-PCR Core Reagents (Applied Biosystems) according to the manufacturer's protocol, using the published primers and probe [44]. The filtered (0.45 μm) culture supernatant of HCV-infected Huh-7 cells containing 2×10^8 HCV RNA copies/ml [equivalent to 9.7×10^4 focus-forming units (ffu)/ml] was used for the experiments. To analyze HCV-RNA in the supernatant, Huh-7 cells (2×10^5 cells in a 6-well plate) were infected with JFH-1 (multiplicity of infection [MOI] = 0.01) and after 4 h the cells were washed twice with phosphate-buffered saline (PBS). The supernatants were then collected and the cells were reseeded at 2×10^5 cells per 6-well plate. Then the HBV expression and mock plasmid were transfected by FuGENE6 (Roche Applied Science, IN, USA). The supernatant of the culture medium was collected 72 h after transfection. Quantification of HBV-DNA and HCV-RNA was carried out using real-time PCR.

IFN-α was added 24 h after the transfection of the HBV plasmids, and the supernatant of the culture medium was then collected 48 h after the addition of the IFN-α.

Results

Clinical characteristics of patients A and B

Patient A (high HBV-DNA titer and high HCV-RNA titer)

Patient A was a 44 year-old man with a high aspartate aminotransferase/alanine aminotransferase (AST/ALT) level. The prothrombin time-international normalized ratio (PT-INR) was in the normal range. Patient A had high HBV-DNA titers and high HCV-RNA titers (Table 1). His liver histology was classified as A2/F3 (Fig. 1). The laparoscopic analysis indicated moderate inflammation and intermediate fibrosis. The liver surfaces of the right lobe and left lobe were almost the same phenotype. Polymorphism of IL-28B (rs8099917) was T/G (hetero allele).

Patient B (low HBV-DNA titer and high HCV-RNA titer)

Patient B was a 63 year-old man with a low AST/ALT level. PT-INR was in the normal range. Patient B had low HBV-DNA titers and high HCV-RNA titers. The liver histology was classified as A2/F1 (Fig. 1). The liver surface showed moderate inflammation and was smooth. The polymorphism of IL-28B (rs8099917) was T/T (major homo allele).

Biopsy samples from patients with dual HBV and HCV infection were collected at the main liver centers in Miyagi prefecture. Fifteen HBV/HCV dual-infected patients were found in this study (Supplementary Table 1). Many of these patients had HCV-dominant infection and undetectable levels of HBV replication (10/15 patients). Most of the patients were HB envelope antigen (eAg)-negative and HBe antibody (Ab)-positive (14/14 patients). All HBV/HCV dual-infected patients who had received Peg-IFN-based

Table 1 Background of HBV/HCV dual-infected patients

	Patient A HCV high titer/ HBV high titer	Patient B HCV high titer/ HBV low titer	Normal range
Gender	Male	Male	
Age (years)	44	63	
HCV-RNA	6.5	5.5	log copies/ml
HCV genotype	1b	1b	
HBV-DNA	5.5	3.5	log copies/ml
HBV genotype	C	Bj	
HBe-Ag	129.5	0.5	0–0.9 index
HBe-Ab	0.1	99.3	0–49 %
Total bilirubin	0.7	1.2	0.2–1.2 mg/dl
Direct bilirubin	0.1	0.1	0–0.3 mg/dl
γ-GTP	208	31	8–57 IU/l
AST	138	33	12–30 IU/l
ALT	256	38	8–35 IU/l
Hb-A1c	5.3	5.4	4.3–5.8 %
Glu	103	83	68–106 mg/dl
BMI	25.34	18.75	
T-cho	160	195	128–220 mg/dl
LDL-cho	69	93	70–139 mg/dl
HDL-cho	37	67	36–89 md/dl
WBC	7800	5100	3200–9600/μl
RBC	491	446	428–566 × 10^4/μl
Hb	17.1	14.1	13.6–17.4 g/dl
PLT	169000	176000	155000–347000/μl
PT-INR	0.87	0.96	0–1.15 INR
Liver histology	A2/F3	A2/F1	METAVIR score
IL-28B SNP (rs8099917)	T/G	T/T	

HCV hepatitis C virus, *HBV* hepatitis B virus, e-*Ag* envelope antigen, *e-Ab* envelope antibody, *γ-GTP* γ-guanosine triphosphate, *AST* aspartate aminotransferase, *ALT* alanine aminotransferase, *Hb* hemoglobin, *Glu* glucose, *BMI* body mass index, *T-cho* total cholesterol, *LDL* low-density lipoprotein, *HDL* high-density lipoprotein, *PLT* platelets, *PT-INR* prothromin time-international normalized ratio, *IL* interleukin, *SNP* single-nucleotide polymorphism

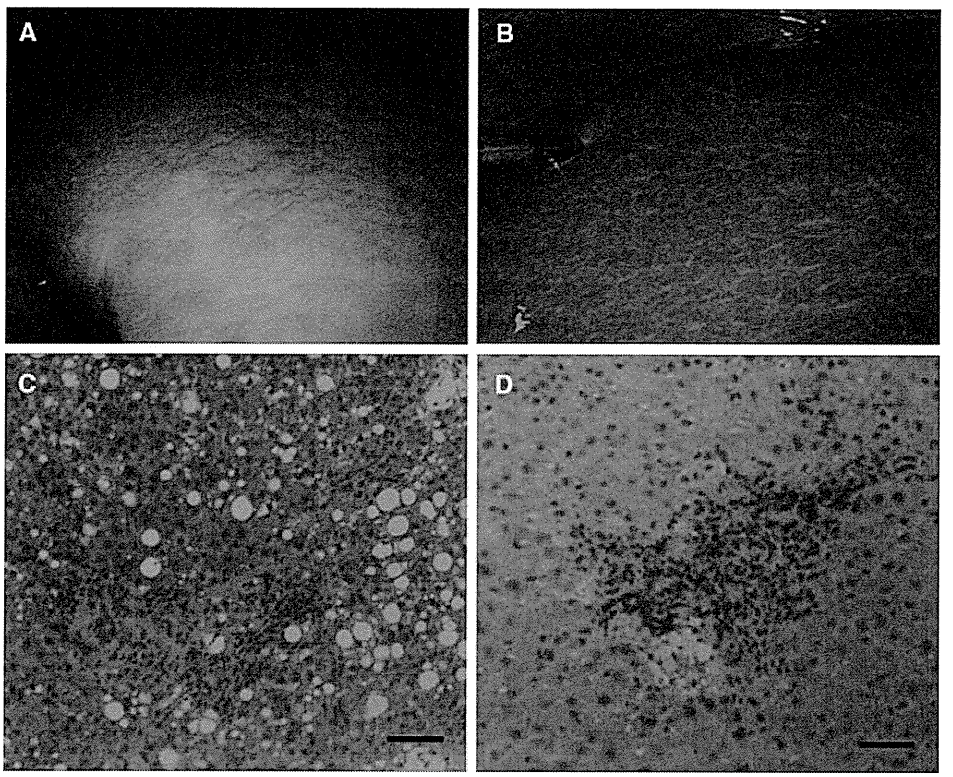

Fig. 1 Laparoscopic liver biopsy. The laparoscopic images of the liver surfaces of patient A (**a**) and patient B (**b**) are shown. Histopathology of patient A (**c**) and patient B (**d**) is also shown. *Bars* = 50 μm

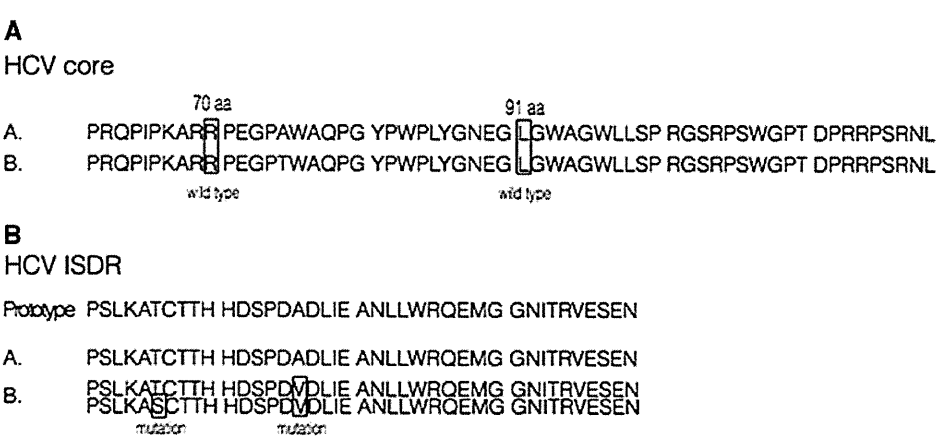

Fig. 2 Virological analysis of hepatitis B virus (HBV) and hepatitis C virus (HCV) in HBV/HCV dual infection. The amino acid sequences of the HCV-core region including core-70 and core-91, which were previously reported as determinants of the sensitivity to pegylated interferon/ribavirin (Peg-IFN/RBV) therapy, in patient A and patient B are shown (**a**). The amino acid sequences of the interferon sensitivity determining region (*ISDR*), which were previously reported as determinants of the sensitivity to IFN, in patients A and B are shown (**b**)

treatment achieved a sustained viral response (SVR) (5/5 patients). These data indicated that HCV-dominant dual-infected patients had good responses to treatment for HCV infection.

Virological analysis of HBV/HCV in patients A and B

The HCV genotype in both patient A and patient B was 1b. The sequences of amino acids in the ISDR region and HCV

core-70 and core-91 amino acids were analyzed by direct sequencing. Both patients had wild-type core-70 and core-91 amino acids (Fig. 2a). None of the mutations of the ISDR region was detected in patient A, but two of the mutations of the ISDR region were detected in patient B (Fig. 2b). The genotypes of HBV in patients A and B were analyzed by direct sequencing and phylogenetic tree analysis. The genotype of HBV in patient A was genotype C, which has been reported as difficult-to-treat HBV. The genotype of HBV in patient B was genotype Bj, which has been reported as easy-to-treat HBV in comparison to genotype C [45–47].

Sequential analysis of biochemical and virological data during Peg-IFN/RBV therapy

Patient A

In patient A, HCV-RNA gradually declined during Peg-IFN/RBV therapy. On the other hand, the HBV-DNA gradually increased during Peg-IFN/RBV therapy (Fig. 3a). The amount of HBeAg started to increase 9 months after the start of Peg-IFN/RBV therapy. HCV-RNA started to increase 12 months after the start of Peg-IFN/RBV therapy, although Peg-IFN/RBV was still being administered up to 18 months after the start of Peg-IFN/RBV therapy (Fig. 3a).

Patient B

In patient B, HCV-RNA and HBV-DNA rapidly declined after the start of Peg-IFN/RBV therapy (Fig. 3b). HCV-RNA could not be detected in peripheral blood 2 months after the start of Peg-IFN/RBV therapy. Peg-IFN/RBV was administered up to 12 months after the start of the Peg-IFN/RBV therapy. The amounts of HBeAb and HBeAg did not change during the Peg-IFN/RBV therapy (Fig. 3b).

Sequential immunological analysis during Peg-IFN/RBV therapy

We analyzed various subsets of immune cells that could affect the immunopathogenesis of HBV/HCV dual infection. NK cells ($CD3^-CD16^-CD56^{high}$ and $CD3^-CD16^+CD56^{dim}$) and NK-T cells ($CD3^+CD56^+CD16^+$, $CD3^+CD56^+CD16^-$ and $CD3^+CD56^-CD16^+$) were analyzed (Supplementary Fig. 1A). The $CD3^-$ gated lymphocytes were separated into 4 groups (a, b, c, and d). For these subsets, (a) indicated the presence of $CD3^-CD16^-CD56^{high}$ NK cells that could produce various cytokines vigorously and had low cytotoxic activity. Subset (b) showed $CD3^-CD16^+CD56^{dim}$ NK cells that had weak cytokine production ability and high cytotoxic activity.

The $CD3^+$ gated lymphocytes were separated into 3 groups (a, b, and c). The activated $CD3^+$, $CD3^+CD4^+$, and $CD3^+CD8^+$ T cells were analyzed (Supplementary Fig. 1B). HLA-DR^+ activated $CD3^+$, $CD3^+CD4^+$, and $CD3^+CD8^+$ T cells could be clearly distinguished by FACS analysis. Additionally, representative dot plots of Tregs and B cells were created (shown in Supplementary Fig. 1C). The frequencies of $CD3^-CD16^+CD56^{dim}$ NK cells, $CD3^+CD16^-CD56^+$ NK-T cells, activated $CD3^+CD4^+$ T cells, and activated $CD3^+CD8^+$ T cells fluctuated similarly during Peg-IFN/RBV therapy in patient A (Supplementary Fig. 1D). Activated T cells were increased at one month of Peg-IFN/RBV therapy, and the above subsets of lymphocytes gradually decreased up to 3 months of Peg-IFN/RBV therapy. After that, these cells gradually increased again up to 9 months of Peg-IFN/RBV therapy. In patient A, after 9 months of Peg-IFN/RBV therapy, these cells had decreased again (Supplementary Fig. 1D). The frequency of Tregs and activated B cells (data not shown) did not change during Peg-IFN/RBV therapy in patient A (Supplementary Fig. 1D). On the other hand, in patient B, the frequencies of $CD3^-CD16^+CD56^{dim}$ NK cells, $CD3^+CD16^-CD56^+$ NK-T cells, activated $CD3^+CD4^+$ T cells, and activated $CD3^+CD8^+$ T cells were increased and sustained during Peg-IFN/RBV therapy (Supplementary Fig. 1E). Five HCV monoinfected patients were analyzed by the same protocol (Supplementary Fig 1F). The mean frequency of various kinds of immune subsets was analyzed (Supplementary Fig 1F). The tendency of immunological reactions during Peg-IFN/RBV therapy in these five patients was similar to that in patient B.

Analysis of HBV- and HCV-specific immune responses

The analysis of HBV- and HCV-specific-immune responses was carried out by ELISPOT assay. Representative spots of IFN-γ are shown in Fig. 4a. In patient A, HCV- and HBV-specific IFN-γ secretion activities were remarkably low in comparison to the IL-10 secretion activity. Moreover, in patient A, the induction of IFN-γ-secreting cells could not be detected after Peg-IFN/RBV therapy, especially in regard to HBV-core specific IFN-γ secretion in PBMCs (Fig. 4b). On the other hand, in patient B, the HBV-core specific IFN-γ-secreting cells were high in comparison to those in patient A (Fig. 4c). Moreover, the induction of IFN-γ-secreting cells could be detected during Peg-IFN/RBV therapy in patient B (Fig. 4c). The mean numbers of IFN-γ- and IL-10-secreting spots in HBV-dominant dual-infected patients, patients with monoinfection with HBV genotype Bj ($HBeAb^+$), Bj ($HBeAg^+$), C ($HBeAb^+$), C ($HBeAg^+$), or HCV genotype 1b are shown in Fig. 4d. In patient A, HB core antigen (HBcAg)-specific IFN-γ secretion was weaker than that in

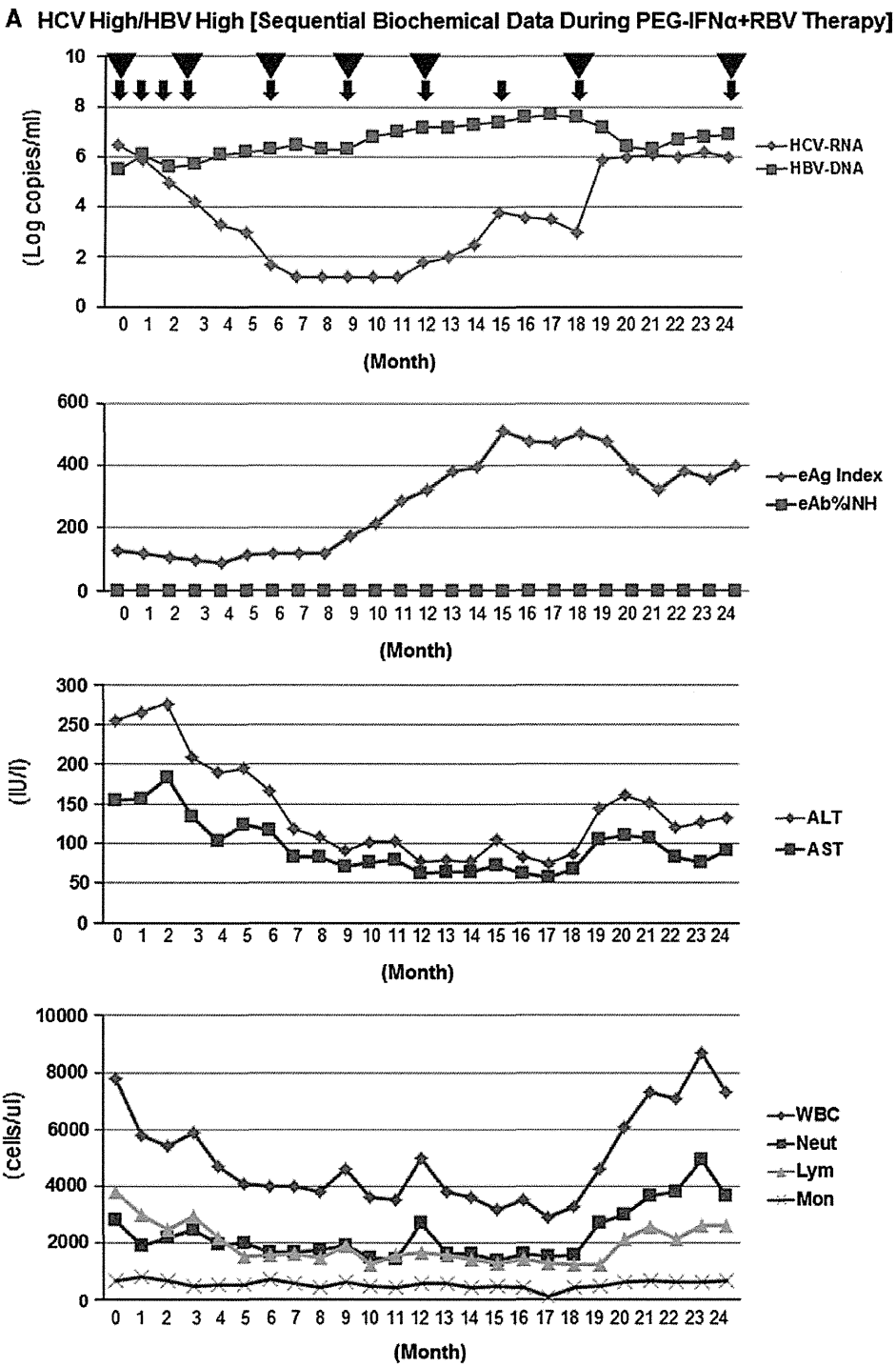

Fig. 3 Sequential biochemical data analysis during Peg-IFN/RBV therapy. The titers of HBV-DNA and HCV-RNA; the amounts of envelope antigen (*eAg*) and envelope antibody (*eAb*), and alanine aminotransferase (*ALT*) and aspartate aminotransferase (*AST*); and the numbers of WBCs, neutrophils (*Neut*), lymphocytes (*Lym*), and monocytes (*Mon*) in patients A (**a**) and B (**b**) are shown in these graphs. *Arrows* indicate the sampling points of FACS analysis. *Triangles* indicate the sampling points of the ELISPOT assay. *INH* inhibition

HBV-genotype C-monoinfected patients who were HBeAg-positive. However, HBcAg-specific IL-10 secretion in patient A was stronger than that in HBV-genotype C monoinfected patients who were HBeAg-positive. These data indicated that the presence of HCV might also suppress the HBV-specific immune response in regard to certain host factors (e.g., in the presence of IL-28B polymorphism, and depending on the body mass index [BMI] and γ-guanosine triphosphate [γ-GTP] level), because the presence of HCV did not suppress the HBV-specific immune response either in patient B or in the patients with dual HCV-dominant infection. Otherwise, we could deny the possibility indicating that

Fig. 3 continued

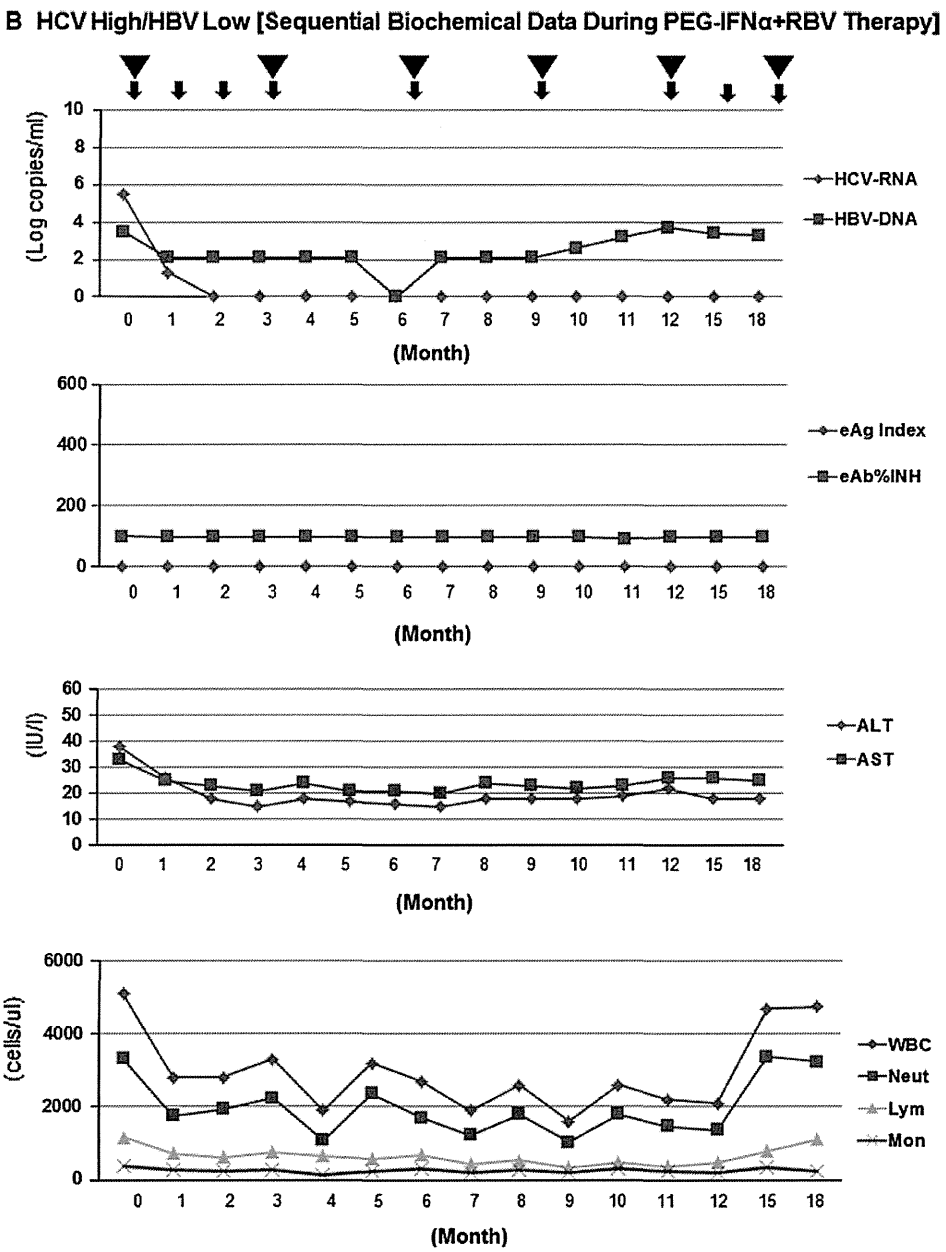

the certain background of host factors could allow the existence of dual virus actively. These data indicated that HBV-specific IL-10-secreting cells and/or certain kinds of host factors had an important role in HBV- and HCV-specific immune suppression in patient A, but not in patient B.

In vitro analysis of HBV/HCV dual infection

We carried out in vitro analysis of HBV/HCV infection using Huh-7 cells that were susceptible to the HCV-JFH-1 strain and HBV expression plasmids. The amount of the JFH-1 strain did not change with the various kinds of HBV expression plasmids (Fig. 5a). Moreover, the amounts of the various HBV strains did not change in the presence of JFH-1 infection. These data indicated that no direct effect of HBV and HCV could be detected in Huh 7 cells. We carried out experiments to analyze the effect of IFN-α treatment on HCV Huh-7 cells with various kinds of HBV expression (Fig. 5b). In our systems, it appeared that HBV expression could not significantly affect the suppressive effect of IFN-α.

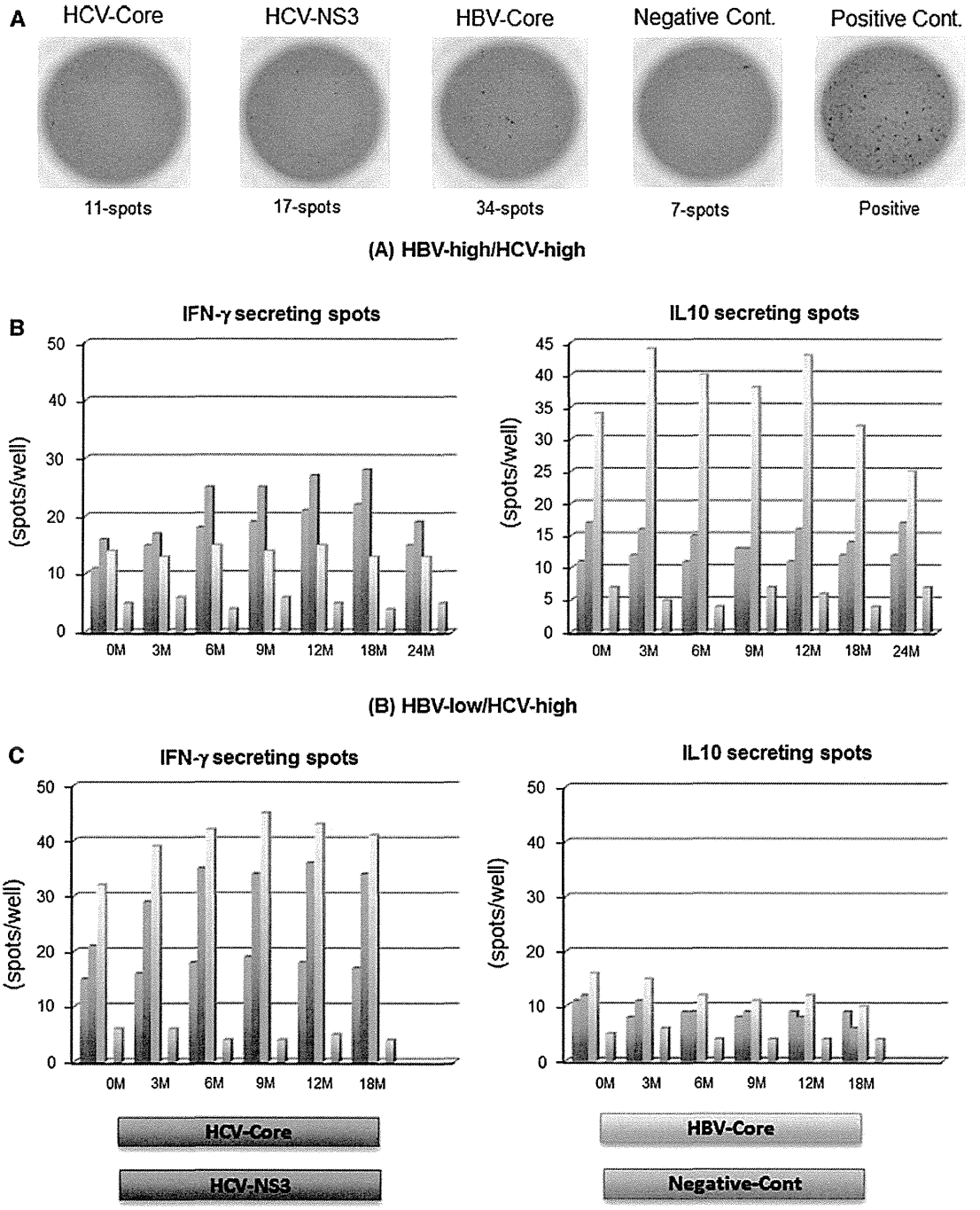

Fig. 4 The sequential analysis of HBV/HCV-specific immune reactions during Peg-IFN/RBV therapy. Representative spots of the ELISPOT assay are shown (**a**). The sequential data of IFN-γ- and interleukin-10 (*IL-10*)- secreting spots in patient A are shown (**b**). The sequential data of IFN-γ- and IL-10-secreting spots in patient B are shown (**c**). Comparison of IFN-γ- and IL-10- secreting spots in patient A before starting therapy, patient B before starting therapy, dual HCV-dominant patients, HCV-monoinfected patients, HBV-Bj ($HBeAb^+$) monoinfected patients, HBV-Bj ($HBeAg^+$) monoinfected patients, HBV-C ($HBeAb^+$) monoinfected patients, and HBV-C ($HBeAg^+$) monoinfected patients (**d**). In these *bar graphs*, the *blue bars* indicate HCV-core specific reaction. The *red bars* indicate HCV-NS3 specific reaction. The *green bars* indicate HBV-core specific reaction. The *aqua blue bars* indicate the negative control (*Cont.*). *Error bars* indicate standard deviations (color figure online)

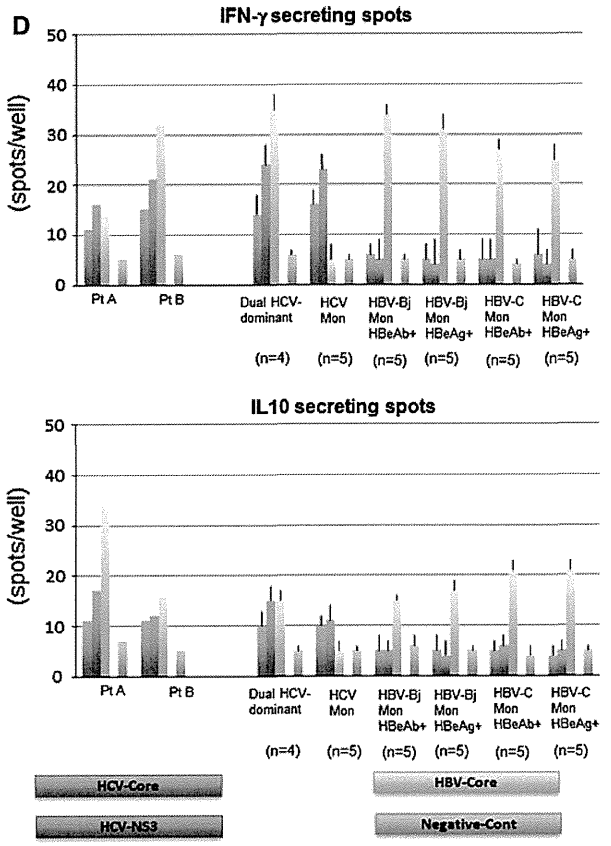

Fig. 4 continued

Discussion

The immunopathogenesis of dual hepatitis B and C infection is not clear, given the complexity of viral and host factors [19, 21, 48–50]. However, detailed understanding of specific patients with dual hepatitis B and C infection could contribute to improving the treatment and follow up of these patients. Therefore, we focused on two representative patients with HBV/HCV dual infection who received Peg-IFN/RBV therapy.

Concerning the virological results, patient A had genotype 1b, HCV-Core 70 wild-type and low mutation of ISDR HCV and genotype C HBV. It has been reported that genotype 1b HCV is common in Japan and is usually difficult to treat in comparison to genotypes 2a and 2b [51]. Among genotype 1b HCV strains, HCV-Core 70 wild-type HCV is easily decreased by Peg-IFN/RBV therapy [51]. On the other hand, it has been reported that in genotype 1b HCV low mutation of ISDR is difficult to treat [52]. Patient B had almost the same background of HCV–genotype 1b, HCV-Core 70 wild-type, and low mutation of ISDR–as patient A. However, the background of host factors that could affect the responsiveness of IFN-based therapy was different between patients A and B. For example, patient A had a hetero allele of the IL-28B polymorphism, advanced fibrosis, and fatty changes of the liver. On the other hand, patient B had the major allele of the IL-28B polymorphism and mild fibrosis. Moreover, the background of HBV in patient B was completely different from that in patient A. It has been reported that HBV genotype Bj is usually more susceptible to IFN-based therapy than genotype C [45, 53]. Therefore, not only the HBV factors but also the combination of host factors and HBV factors might affect the responsiveness to IFN-based therapy. In patient A, the responsiveness of HCV during Peg-IFN/RBV therapy was relatively poor. However, the viral titers of HCV were lower than 1.2 log copies/ml at 7 months after the start of therapy. During the reduction of the HCV viral titers, the titers of HBV and HBc-Ag specific IL-10-secreting cells were gradually increased. Although patient A had received Peg-IFN/RBV therapy for up to 18 months, HCV-RNA increased again 12 months after the start of the therapy. The sustained Th1 immune suppression might have contributed to the relapse of HCV. Not only weak up-regulation of HCV-specific Th1 immune reaction but also strong up-regulation of HBV-specific IL-10-secreting activity was detected during Peg-IFN/RBV therapy in patient A [26, 35]. Moreover, increased HBeAg could be detected 9 months after the start of the therapy. Fluctuations of activated CD4 cells, CD8 cells, NK cells, and NK-T cells could be seen in patient A. On the other hand, in patient B, the responsiveness of HBV and HCV during Peg-IFN/RBV therapy was good. Moreover, the immune response of patient B was almost comparable to the responses in the patients with HCV monoinfection and those with HBV-genotype Bj monoinfection. Previously, it has been reported that Peg-IFN/RBV therapy could achieve almost the same SVR rates in patients with HCV/HBV dual infection and those with HCV monoinfection [54–56]. We assume that the results in these studies were obtained from patients similar to our patient B, because the number of patients with HCV-dominant infection is much higher than the number of those with HBV/HCV dual active infection such as our patient A. Patients with HBV/HCV dual active infection such as patient A are relatively rare in Japan. However, it is necessary to understand the immunopathogenesis of these patients, because Peg-IFN/RBV therapy might not be sufficient to eradicate or control HBV/HCV in these difficult-to-treat patients. One of the candidate therapies for such patients might be Entecavir (ETV)/Peg-IFN/RBV sequential therapy. The effect of HBV specific regulatory T cells might contribute to the immunosuppression of not only HBV but also HCV [35]. In some previous studies, including ours, it has been reported that HBV replication might contribute to immune suppression [19, 29].

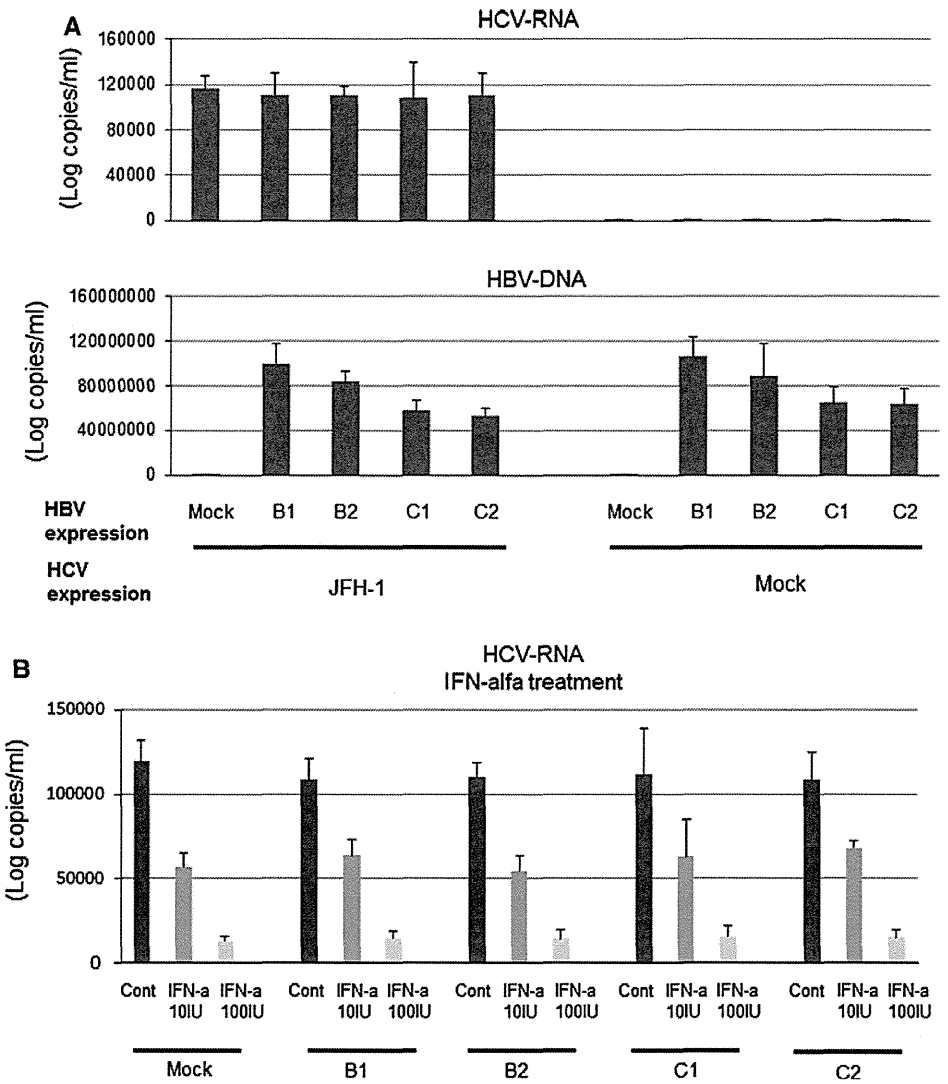

Fig. 5 In vitro analysis of HBV/HCV dual infection. The titers of HCV-RNA and HBV-DNA are shown. *B1* indicates genotype Bj35 clone. *B2* indicates genotype Bj56 clone. *C1* indicates genotype C-AT clone. *C2* indicates genotype C-22 clone (**a**). The titers of HCV-RNA after the IFN-α treatment are shown (**b**)

In the present study, we employed an in vitro coinfection system to analyze the direct interaction between HBV and HCV. In our system, we used several different HBV clones, because it is necessary to consider the effects of different genotypes. Although we could not detect the direct interaction of HBV/HCV in our system, we could not exclude the possibility of indirect interaction between cytokines and chemokines produced from virus-infected hepatocytes. We are now analyzing the chemokines produced from hepatoma cells with different HBV genotype clones (ongoing study).

In conclusion, we analyzed data from representative patients with HBV/HCV dual infection sequentially and precisely. Because many different kinds of backgrounds might affect immunoreactions, we focused on representative patients and analyzed the immunological responses extensively. There might be a group of patients with very difficult-to-treat dual infections. We need to understand the immunopathogenesis of such patients to develop the appropriate therapy.

Acknowledgments This work was supported in part by a Grant-in Aid from the Ministry of Education, Culture, Sport, Science, and Technology of Japan (Y.K. #23790761), and grants from the Ministry of Health, Labor, and Welfare of Japan.

Conflict of interest The authors declare that they have no conflict of interest.

References

1. Alter MJ, Kruszon-Moran D, Nainan OV, et al. The prevalence of hepatitis C virus infection in the United States, 1988 through 1994. N Engl J Med. 1999;341(8):556–62.

2. Tiollais P, Pourcel C, Dejean A. The hepatitis B virus. Nature. 1985;317(6037):489–95.
3. Lai CL, Ratziu V, Yuen MF, Poynard T. Viral hepatitis B. Lancet. 2003;362(9401):2089–94.
4. Poynard T, Yuen MF, Ratziu V, Lai CL. Viral hepatitis C. Lancet. 2003;362(9401):2095–100.
5. Potthoff A, Manns MP, Wedemeyer H. Treatment of HBV/HCV coinfection. Expert Opin Pharmacother. 2010;11(6):919–28.
6. Chu CJ, Lee SD. Hepatitis B virus/hepatitis C virus coinfection: epidemiology, clinical features, viral interactions and treatment. J Gastroenterol Hepatol. 2008;23(4):512–20.
7. Bini EJ, Perumalswami PV. Hepatitis B virus infection among American patients with chronic hepatitis C virus infection: prevalence, racial/ethnic differences, and viral interactions. Hepatology. 2010;51(3):759–66.
8. Halima SB, Bahri O, Maamouri N, et al. Serological and molecular expression of hepatitis B infection in patients with chronic hepatitis C from Tunisia, North Africa. Virol J. 2010;7:229.
9. Saravanan S, Velu V, Nandakumar S, et al. Hepatitis B virus and hepatitis C virus dual infection among patients with chronic liver disease. J Microbiol Immunol Infect. 2009;42(2):122–8.
10. Lee LP, Dai CY, Chuang WL, et al. Comparison of liver histopathology between chronic hepatitis C patients and chronic hepatitis B and C-coinfected patients. J Gastroenterol Hepatol. 2007;22(4):515–7.
11. Liu Z, Hou J. Hepatitis B virus (HBV) and hepatitis C virus (HCV) dual infection. Int J Med Sci. 2006;3(2):57–62.
12. Tsai JF, Jeng JE, Ho MS, et al. Effect of hepatitis C and B virus infection on risk of hepatocellular carcinoma: a prospective study. Br J Cancer. 1997;76(7):968–74.
13. Cho LY, Yang JJ, Ko KP, et al. Coinfection of hepatitis B and C viruses and risk of hepatocellular carcinoma: systematic review and meta-analysis. Int J Cancer. 2011;128(1):176–84.
14. Huo TI, Huang YH, Hsia CY, et al. Characteristics and outcome of patients with dual hepatitis B and C-associated hepatocellular carcinoma: are they different from patients with single virus infection? Liver Int. 2009;29(5):767–73.
15. Kew MC. Interaction between hepatitis B and C viruses in hepatocellular carcinogenesis. J Viral Hepat. 2006;13(3):145–9.
16. Liu CJ, Chen PJ, Chen DS. Dual chronic hepatitis B virus and hepatitis C virus infection. Hepatol Int. 2009;3(4):517–25.
17. Bellecave P, Gouttenoire J, Gajer M, et al. Hepatitis B and C virus coinfection: a novel model system reveals the absence of direct viral interference. Hepatology. 2009;50(1):46–55.
18. Eyre NS, Phillips RJ, Bowden S, et al. Hepatitis B virus and hepatitis C virus interaction in Huh-7 cells. J Hepatol. 2009;51(3):446–57.
19. Chisari FV, Ferrari C. Hepatitis B virus immunopathogenesis. Annu Rev Immunol. 1995;13:29–60.
20. Koziel MJ. The role of immune responses in the pathogenesis of hepatitis C virus infection. J Viral Hepat. 1997;4(Suppl 2):31–41.
21. Rice CM, Walker CM. Hepatitis C virus-specific T lymphocyte responses. Curr Opin Immunol. 1995;7(4):532–8.
22. Nan XP, Zhang Y, Yu HT, et al. Circulating $CD4^{+}CD25^{high}$ regulatory T cells and expression of PD-1 and BTLA on $CD4^{+}$ T cells in patients with chronic hepatitis B virus infection. Viral Immunol. 2010;23(1):63–70.
23. Kondo Y, Ueno Y, Shimosegawa T. Immunopathogenesis of hepatitis B persistent infection: implications for immunotherapeutic strategies. Clin J Gastroenterol. 2009;2(2):71–9.
24. Peng G, Li S, Wu W, Sun Z, Chen Y, Chen Z. Circulating $CD4^{+}$ $CD25^{+}$ regulatory T cells correlate with chronic hepatitis B infection. Immunology. 2008;123(1):57–65.
25. Maier H, Isogawa M, Freeman GJ, Chisari FV. PD-1:PD-L1 interactions contribute to the functional suppression of virus-specific $CD8^{+}$ T lymphocytes in the liver. J Immunol. 2007;178(5):2714–20.
26. Kondo Y, Kobayashi K, Ueno Y, et al. Mechanism of T cell hyporesponsiveness to HBcAg is associated with regulatory T cells in chronic hepatitis B. World J Gastroenterol. 2006;12(27):4310–7.
27. Stoop JN, van der Molen RG, Baan CC, et al. Regulatory T cells contribute to the impaired immune response in patients with chronic hepatitis B virus infection. Hepatology. 2005;41(4):771–8.
28. Kondo Y, Kobayashi K, Asabe S, et al. Vigorous response of cytotoxic T lymphocytes associated with systemic activation of CD8 T lymphocytes in fulminant hepatitis B. Liver Int. 2004;24(6):561–7.
29. Kondo Y, Asabe S, Kobayashi K, et al. Recovery of functional cytotoxic T lymphocytes during lamivudine therapy by acquiring multi-specificity. J Med Virol. 2004;74(3):425–33.
30. Kondo Y, Ueno Y, Kakazu E, et al. Lymphotropic HCV strain can infect human primary naive CD4(+) cells and affect their proliferation and IFN-gamma secretion activity. J Gastroenterol. 2011;46:232–41.
31. Kondo Y, Machida K, Liu HM, et al. Hepatitis C virus infection of T cells inhibits proliferation and enhances fas-mediated apoptosis by down-regulating the expression of CD44 splicing variant 6. J Infect Dis. 2009;199(5):726–36.
32. Kondo Y, Sung VM, Machida K, Liu M, Lai MM. Hepatitis C virus infects T cells and affects interferon-gamma signaling in T cell lines. Virology. 2007;361(1):161–73.
33. Ulsenheimer A, Gerlach JT, Gruener NH, et al. Detection of functionally altered hepatitis C virus-specific CD4 T cells in acute and chronic hepatitis C. Hepatology. 2003;37(5):1189–98.
34. Cramp ME, Rossol S, Chokshi S, Carucci P, Williams R, Naoumov NV. Hepatitis C virus-specific T-cell reactivity during interferon and ribavirin treatment in chronic hepatitis C. Gastroenterology. 2000;118(2):346–55.
35. Kondo Y, Ueno Y, Kobayashi K, et al. Hepatitis B virus replication could enhance regulatory T cell activity by producing soluble heat shock protein 60 from hepatocytes. J Infect Dis. 2010;202(2):202–13.
36. Nguyen LH, Ko S, Wong SS, et al. Ethnic differences in viral dominance patterns in patients with hepatitis B virus and hepatitis C virus dual infection. Hepatology. 2011;53(6):1839–45.
37. Takahashi M, Nishizawa T, Gotanda Y, et al. High prevalence of antibodies to hepatitis A and E viruses and viremia of hepatitis B, C, and D viruses among apparently healthy populations in Mongolia. Clin Diagn Lab Immunol. 2004;11(2):392–8.
38. Ina Y. ODEN: a program package for molecular evolutionary analysis and database search of DNA and amino acid sequences. Comput Appl Biosci. 1994;10(1):11–2.
39. Thompson JD, Higgins DG, Gibson TJ. CLUSTAL W: improving the sensitivity of progressive multiple sequence alignment through sequence weighting, position-specific gap penalties and weight matrix choice. Nucleic Acids Res. 1994;22(22):4673–80.
40. Saitou N, Nei M. The neighbor-joining method: a new method for reconstructing phylogenetic trees. Mol Biol Evol. 1987;4(4):406–25.
41. Felsenstein J. Estimating effective population size from samples of sequences: a bootstrap Monte Carlo integration method. Genet Res. 1992;60(3):209–20.
42. Perriere G, Gouy M. WWW-query: an on-line retrieval system for biological sequence banks. Biochimie. 1996;78(5):364–9.
43. Wakita T, Pietschmann T, Kato T, et al. Production of infectious hepatitis C virus in tissue culture from a cloned viral genome. Nat Med. 2005;11(7):791–6.
44. Takeuchi T, Katsume A, Tanaka T, et al. Real-time detection system for quantification of hepatitis C virus genome. Gastroenterology. 1999;116(3):636–42.

45. Sugauchi F, Kumada H, Sakugawa H, et al. Two subtypes of genotype B (Ba and Bj) of hepatitis B virus in Japan. Clin Infect Dis. 2004;38(9):1222–8.
46. Sugauchi F, Orito E, Ichida T, et al. Epidemiologic and virologic characteristics of hepatitis B virus genotype B having the recombination with genotype C. Gastroenterology. 2003; 124(4):925–32.
47. Orito E, Mizokami M, Sakugawa H, et al. A case–control study for clinical and molecular biological differences between hepatitis B viruses of genotypes B and C. Japan HBV Genotype Research Group. Hepatology. 2001;33(1):218–23.
48. Raimondo G, Brunetto MR, Pontisso P, et al. Longitudinal evaluation reveals a complex spectrum of virological profiles in hepatitis B virus/hepatitis C virus-coinfected patients. Hepatology. 2006;43(1):100–7.
49. Chuang WL, Dai CY, Chang WY, et al. Viral interaction and responses in chronic hepatitis C and B coinfected patients with interferon-alpha plus ribavirin combination therapy. Antivir Ther. 2005;10(1):125–33.
50. Tsai SL, Liaw YF, Yeh CT, Chu CM, Kuo GC. Cellular immune responses in patients with dual infection of hepatitis B and C viruses: dominant role of hepatitis C virus. Hepatology. 1995;21(4):908–12.
51. Akuta N, Suzuki F, Hirakawa M, et al. Amino acid substitution in hepatitis C virus core region and genetic variation near the interleukin 28B gene predict viral response to telaprevir with peginterferon and ribavirin. Hepatology. 2010;52(2):421–9.
52. Fukuma T, Enomoto N, Marumo F, Sato C. Mutations in the interferon-sensitivity determining region of hepatitis C virus and transcriptional activity of the nonstructural region 5A protein. Hepatology. 1998;28(4):1147–53.
53. Akuta N, Kumada H. Influence of hepatitis B virus genotypes on the response to antiviral therapies. J Antimicrob Chemother. 2005;55(2):139–42.
54. Yu ML, Lee CM, Chuang WL, et al. HBsAg profiles in patients receiving peginterferon alfa-2a plus ribavirin for the treatment of dual chronic infection with hepatitis B and C viruses. J Infect Dis. 2010;202(1):86–92.
55. Yu JW, Sun LJ, Zhao YH, Kang P, Gao J, Li SC. Analysis of the efficacy of treatment with peginterferon alpha-2a and ribavirin in patients coinfected with hepatitis B virus and hepatitis C virus. Liver Int. 2009;29(10):1485–93.
56. Liu CJ, Chuang WL, Lee CM, et al. Peginterferon alfa-2a plus ribavirin for the treatment of dual chronic infection with hepatitis B and C viruses. Gastroenterology. 2009;136((2)):496.e3–504.e3.

Genes **2014**, *5*, 84-96; doi:10.3390/genes5010084

OPEN ACCESS

genes

ISSN 2073-4425

www.mdpi.com/journal/genes

Review

Lessons from Genome-Wide Search for Disease-Related Genes with Special Reference to HLA-Disease Associations

Katsushi Tokunaga

Department of Human Genetics, Graduate School of Medicine, University of Tokyo, Tokyo 113-0013, Japan; E-Mail: tokunaga@m.u-tokyo.ac.jp

Received: 8 January 2014; in revised form: 11 February 2014 / Accepted: 12 February 2014 / Published: 26 February 2014

Abstract: The relationships between diseases and genetic factors are by no means uniform. Single-gene diseases are caused primarily by rare mutations of specific genes. Although each single-gene disease has a low prevalence, there are an estimated 5000 or more such diseases in the world. In contrast, multifactorial diseases are diseases in which both genetic and environmental factors are involved in onset. These include a variety of diseases, such as diabetes and autoimmune diseases, and onset is caused by a range of various environmental factors together with a number of genetic factors. With the astonishing advances in genome analysis technology in recent years and the accumulation of data on human genome variation, there has been a rapid progress in research involving genome-wide searches for genes related to diseases. Many of these studies have led to the recognition of the importance of the human leucocyte antigen (HLA) gene complex. Here, the current state and future challenges of genome-wide exploratory research into variations that are associated with disease susceptibilities and drug/therapy responses are described, mainly with reference to our own experience in this field.

Keywords: genome-wide association study (GWAS); multifactorial disease; disease susceptibility gene; drug response gene; HLA genes

1. Development of Genome-Wide Searches

The greatest attraction of the strategy of genome-wide searches for genes related to diseases is the potential for the discovery of the involvement of completely new genes that could not have been predicted using existing knowledge or data. The previous method for genome-wide search of

multifactorial disease-susceptibility genes was non-parametric linkage analysis, which does not presuppose any specific inheritance mode. One such method is the affected sib-pair method. However, it is not easy to collect a large number of samples with affected sib-pairs, so the detection power of this method is inevitably low [1]. Consequently, only limited results have been obtained so far.

The genome-wide association study (GWAS), however, makes use of the high statistical power of association analysis traditionally used for investigating the possible involvement of specific candidate genes, and applies it genome-wide [1]. Two pioneering GWAS studies were carried out in Japan. One was the first single nucleotide polymorphism (SNP)-based GWAS for myocardial infarction, which utilized an approximately 90,000 SNPs [2]. The other was the first microsatellite-based GWAS for rheumatoid arthritis, which used approximately 30,000 microsatellite polymorphisms [3]. However, only a few research groups adopted either of these platforms, due to the labor and cost they involved.

GWAS advanced to a new stage from 2006 onward, mainly as a result of two developments in infrastructure. The first was information infrastructure, typified by the Database of Single Nucleotide Polymorphisms (dbSNP) [4], the International HapMap Project [5] and the 1000 Genomes Project [6], which gathered together a vast range of information of genome variation that spanned the entire human genome. The other development was in technology infrastructure; this was the commercial release of platforms that allowed the analysis of several thousands of samples performed on several hundreds of thousands of SNPs and could be carried out relatively easily. The application of these developments meant that SNP-based GWAS became a broad-based, practical strategy, and in 2007, several studies were published from large-scale collaborations between multiple institutions. The subsequent rush to discover gene polymorphisms associated with different diseases or traits using GWAS was dramatic, and over 1600 types of significant associations with 250 diseases or traits have been reported [7]. Nevertheless, attention should be paid for GWAS in ethnically diverse populations, since the genome-wide SNP typing chips have been designed based on mainly European data, these chips may have limited utility in certain populations.

2. Identified Susceptibility Genes to Multifactorial Diseases

2.1. Population Differences in Disease Susceptibility Genes

A disease for which GWAS have shown striking results is type II diabetes. In 2007, several groups from Europe and North America reported results from different GWAS on several thousand patients and controls [8–11]. Over 11 susceptibility loci were identified, and over half of these were newly discovered. The following year, two independent groups from Japan reported a new susceptibility gene, *KCNQ1* [12,13]. Table 1 shows a comparison between European and Japanese populations of the allele frequency, odds ratio and *p*-value of *TCF7L2*, the most important susceptibility gene found in European populations, and *KCNQ1*, which was discovered in Japanese. *TCF7L2* showed a *p*-value of 10^{-48} in European populations, indicating a definite association with type II diabetes [8]. Among Japanese, however, the *p*-value is at a level of no more than 10^{-4} [14]. The main reason for this is the difference in minor allele frequency, which is lower in Japanese by an order of magnitude. Consequently, although the odds ratio is similar to European populations, no clear association was observed in an analysis of 2000 patients and 2000 healthy controls. A contrasting relationship can be seen with *KCNQ1* [12]. The